Fredericq, E. (1956) *Arch. Biochem. Biophys. 65*, 218-228.
Geary, W. J., Nickless, G., & Pollard, F. H. (1962) *Anal. Chim. Acta 27*, 71-79.
Goldman, J., & Carpenter, F. H. (1974) *Biochemistry 13*, 4566-4574.
Grant, P. T., Combs, T. L., & Frank, B. H. (1972) *Biochem. J. 126*, 433-440.
Howell, S. L., Montague, W., & Tyhurst, M. (1985) *J. Cell Sci. 19*, 395-409.
Jeffrey, P. D. (1974) *Biochemistry 13*, 4441-4447.
Jeffrey, P. D., & Coates, J. H. (1966) *Biochemistry 5*, 489-498.
Jeffrey, P. D., Milthorpe, B. K., & Nichol, L. W. (1976) *Biochemistry 15*, 4660-4665.
Marcker, K. (1960) *Acta Chem. Scand. 14*, 2071-2074.
Milthorpe, B. K., Nichol, L. W. & Jeffrey, P. D. (1977) *Biochim. Biophys. Acta 495*, 195-202.
Ohyoshi, E. (1983) *Anal. Chem. 55*, 2404-2407.
Pekar, A. H., & Frank, B. H. (1972) *Biochemistry 11*, 4013.
Peking Insulin Structure Research Group (1974) *Sci. Sin. (Engl. Ed.) 17*, 779-792.
Pocker, Y., & Biswas, S. B. (1981) *Biochemistry 20*, 4354-4361.
Porter, R. R. (1953) *Biochem. J. 53*, 320-328.
Reinscheidt, H., Strassburger, W., Glatter, U., Wollmer, A., Dodson, G. G., & Mercola, D. A. (1984) *Eur. J. Biochem. 142*, 7-14.
Sakabe, N., Sakabe, K., & Sasaki, K. (1981) in *Structural Studies on Molecules of Biological Interest* (Dodson, G., Glusker, J. P., & Sayre, D., Eds.) pp 509-526, Clarendon Press, Oxford University Press, London.
Schlichtkrull, J. (1956) *Acta Chem. Scand. 10*, 1455-1458.
Storm, M. C., & Dunn, M. F. (1985) *Biochemistry 24*, 1749-1756.
Sudmeier, J. L., Bell, S. J., Storm, M. C., & Dunn, M. F. (1981) *Science (Washington, D.C.) 212*, 560-562.
Tanaka, M., Funahashi, S., & Shirai, K. (1968) *Inorg. Chem. 7*, 573-578.

^{1}H NMR Aromatic Spectrum of the Operator Binding Domain of the λ Repressor: Resonance Assignment with Application to Structure and Dynamics†

Michael A. Weiss,‡,§ Martin Karplus,*,‡ and Robert T. Sauer‖

Department of Chemistry, Harvard University, Cambridge, Massachusetts 02138, Department of Medicine, Brigham and Women's Hospital, Boston, Massachusetts 02115, and Department of Biology, Massachusetts Institute of Technology, Cambridge, Massachusetts 02139

Received June 10, 1986; Revised Manuscript Received September 19, 1986

ABSTRACT: The aromatic ^{1}H NMR resonances of the operator binding domain of λ repressor are completely assigned. Since the resonances of this 23-kilodalton domain are too broad for the application of two-dimensional strategies for sequence-specific assignment, an alternative approach has been used. Assignments are obtained by a combination of one- and two-dimensional NMR methods, by the study of genetically altered domains, and by the biosynthetic incorporation of deuterium labels. The resulting assignments provide sensitive markers for tertiary and quaternary structure. Nuclear Overhauser enhancements demonstrate that the major features of the crystal structure, including the dimer contacts, are retained in solution. The rates of aromatic ring rotation indicate that the globular domain is not rigid; significant barriers to ring rotation are observed only in the dimer contact.

The λ repressor contains two domains, which have distinct functions (Pabo et al., 1979; Sauer et al., 1979). The N-terminal domain recognizes operator DNA, and the C-terminal domain contains strong dimer and higher order contacts. In the intact protein, the two domains are dynamically independent (Weiss et al., 1983). Several other prokaryotic repressors have a similar pattern of domain organization (Platt et al., 1973; Weber & Geisler, 1978; DeAnda et al., 1983; Anderson et al., 1984; Little et al., 1985).

The structure of the N-terminal domain of λ repressor has been determined by X-ray crystallography (Pabo & Lewis, 1982). Consisting of residues 1-92, this domain contains five α-helices, as shown in panel A of Figure 1. The first four helices form a globular domain, and the fifth extends outward to form a dimer contact. In the primary sequence of the N-terminal domain, there are four tyrosines and two phenylalanines (Sauer & Anderegg, 1978). These are shown in panel B of Figure 1. Three tyrosines (Tyr-60, Tyr-85, and Tyr-88) are on the surface of the monomer, and the fourth (Tyr-22) is in the interior of the domain. Both phenylalanines Phe-51 and Phe-76) are internal.

The dimer structure found in the crystal is shown in panel C of Figure 1. The fifth helix of one protomer packs against the symmetry-related helix from the other protomer. These helices are amphipathic, and the packing is primarily hydrophobic. Dimerization alters the environments of the three surface tyrosines. Tyr-88 is buried in the dimer interface, where it stacks against Tyr-88′ from the other protomer. Tyr-60 and Tyr-85 remain on the surface of the dimer but are near side chains from the other protomer.

In this paper we focus on a dimeric fragment consisting of residues 1-102. This fragment contains an additional tyrosine, Tyr-101, which is shown to be in a random-coil state. The aromatic proton resonances are assigned by a combination of one- and two-dimensional NMR methods, by the study of genetic variants, and by the biosynthetic incorporation of

† This work was supported in part by grants from the National Institutes of Health to M.K. (GM-37292) and R.T.S. (AI-15706).
‡ Harvard University.
§ Brigham and Women's Hospital.
‖ Massachusetts Institute of Technology.

0006-2960/87/0426-0890$01.50/0

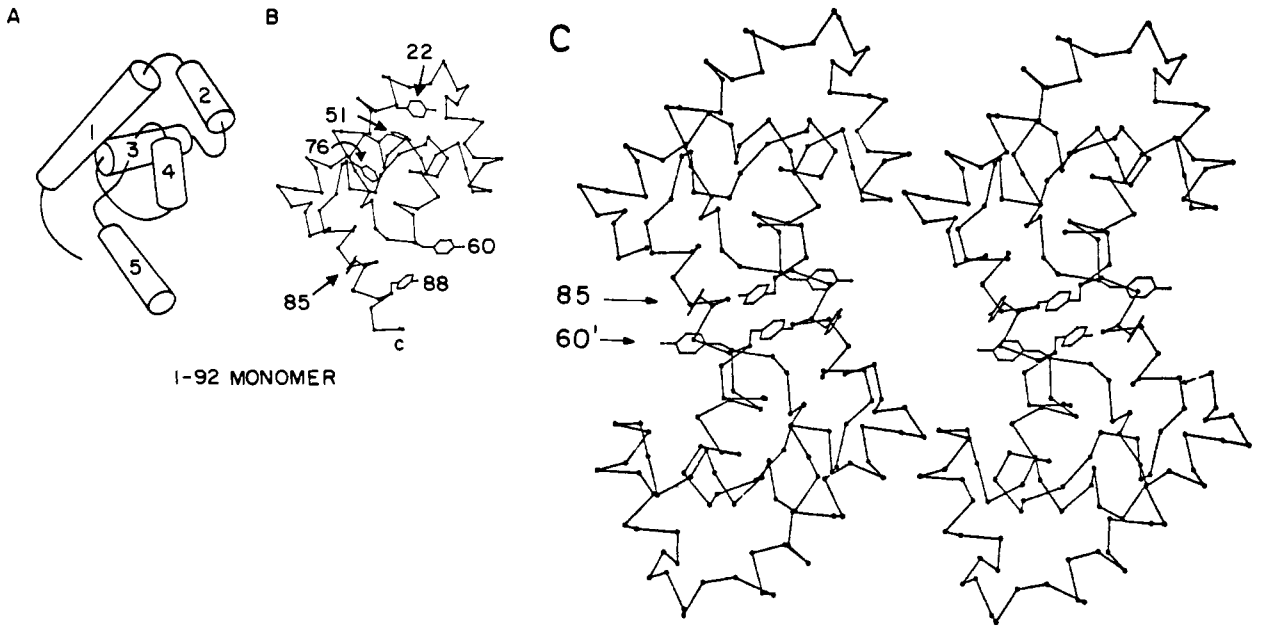

FIGURE 1: (A) Model of the 1–92 domain of phage λ repressor. The α-helices are shown as cylinders. The first four helices form a globular region, and the fifth extends outward. (B) α-Carbon representation showing aromatic side chains. Tyr-22, Phe-51, and Phe-76 are buried in the hydrophobic interior and provide sensitive markers for changes in tertiary structure. Tyr-60, Tyr-85, and Tyr-88 are on the surface. Their environments are altered in the dimer. (C) Stereopair showing helix 5–helix 5 interaction. Tyr-88 stacks against Tyr-88′ in the dimer interface and also comes within 4 Å of Tyr-85′. The structures were calculated from the crystal coordinates (Pabo & Lewis, 1982).

deuterium labels. The assignments are then utilized to evaluate certain structural and dynamic features of the N-terminal domain.

Materials and Methods

The wild-type 1–102 fragment and mutant fragments were purified from overproducing strains of *Escherichia coli* as described (Sauer et al., 1986). The 5–98 fragment was obtained by limited proteolysis of intact repressor by clostripain and provided by C. O. Pabo.

Deuterated tyrosine was purchased from Merck Sharp & Dohme, Ltd. Partially deuterated phenylalanine was provided by Dr. Robert Griffin (Massachusetts Institute of Technology). Biosynthetic incorporation was accomplished by the method of Lu and co-workers (Jarema et al., 1981).

^{1}H NMR spectra were obtained at 500 MHz as described (Weiss et al., 1984). One-dimensional nuclear Overhauser effects were measured by the technique of Redfield (Gupta & Redfield, 1971). Two-dimensional spectra were obtained by the pure-phase method (Aue et al., 1976; States et al., 1982). For NMR study, the proteins were exhaustively dialyzed against distilled, deionized water containing 50 mM ammonium bicarbonate and lyophilized. The powder was dissolved in 99.8% D_2O, lyophilized, dissolved in 340 μL of NMR buffer, and placed in a 5-mm NMR tube. The protein concentration was 5 mM, assuming that a 1 mg/mL solution of the 1–102 fragment has an absorbance of 0.62 cm^{-1} at 280 nm. NMR buffer consists of 200 mM KCl, 50 mM potassium phosphate (pD 7.4, direct meter reading), 1 mM sodium azide, and 0.1 mM ethylenediaminetetraacetic acid (EDTA) in 99.98% D_2O.

Results

The aromatic region of the ^{1}H NMR spectrum of the 1–102 fragment is shown in panel A of Figure 2. The fragment is essentially dimeric at the concentration and conditions used (Weiss et al., 1987). The molecular weight of the dimer is 23 000, and its resonances are broad. There is a marked dispersion in chemical shifts, reflecting the variety of magnetic environments in the native structure. As a first step in characterizing this spectrum, individual resonances are classified by type (e.g., meta resonances of tyrosine). Next, these resonances are assigned to particular residues in the protein.

Classification of ^{1}H NMR resonances by type may be accomplished by selective deuterium labeling. For example, the aromatic spectrum of a domain containing 70% [2′,3′,4′,5′,6′-$^2H_5$]phenylalanine is shown in panel B of Figure 2. A number of resonances are proportionately reduced in amplitude. These are assigned to the two phenylalanine residues. Similarly, panel C contains the aromatic spectrum of a domain 94% enriched with [*m*-$^2H_2$]tyrosine. Consequently, these resonances are virtually absent from the spectrum, and the unlabeled ortho resonances of tyrosine appear as singlets instead of (unresolved) doublets. The aromatic spectrum of a domain labeled with [*o*-$^2H_2$]tyrosine is shown in panel D. In each case the positions of the ^{1}H resonances corresponding to the deuterated position are designated by arrows in the appropriate panel.

This classification is confirmed and extended by the application of two-dimensional correlated methods (Jeener, 1971; Aue et al., 1976; Wüthrich et al., 1982). Such methods delineate *J* connectivities and so may be used to identify individual spin systems. Because of their different covalent structures, tyrosine and phenylalanine give rise to different patterns of two-dimensional resonances. The correlated spectrum of the 1–102 domain contains four tyrosine and two phenylalanine spin systems, all in fast exchange about the C_β–C_γ bond axis from 0 to 30 °C (data not shown). These spin systems are outlined in Figure 3. One tyrosine (Tyr-88; see below), identifiable by deuterium labeling, does not appear in the two-dimensional spectrum. Its *J* connectivity is absent in the two-dimensional spectrum because its ortho resonances are broadened by intermediate exchange.

We next assign these resonances to particular residues in the protein. Because the sequence-specific methods developed in studies of bovine pancreatic trypsin inhibitor (Wüthrich et al., 1982; Wagner & Wüthrich, 1982) are difficult to apply to this system, we will consider each aromatic residue indi-

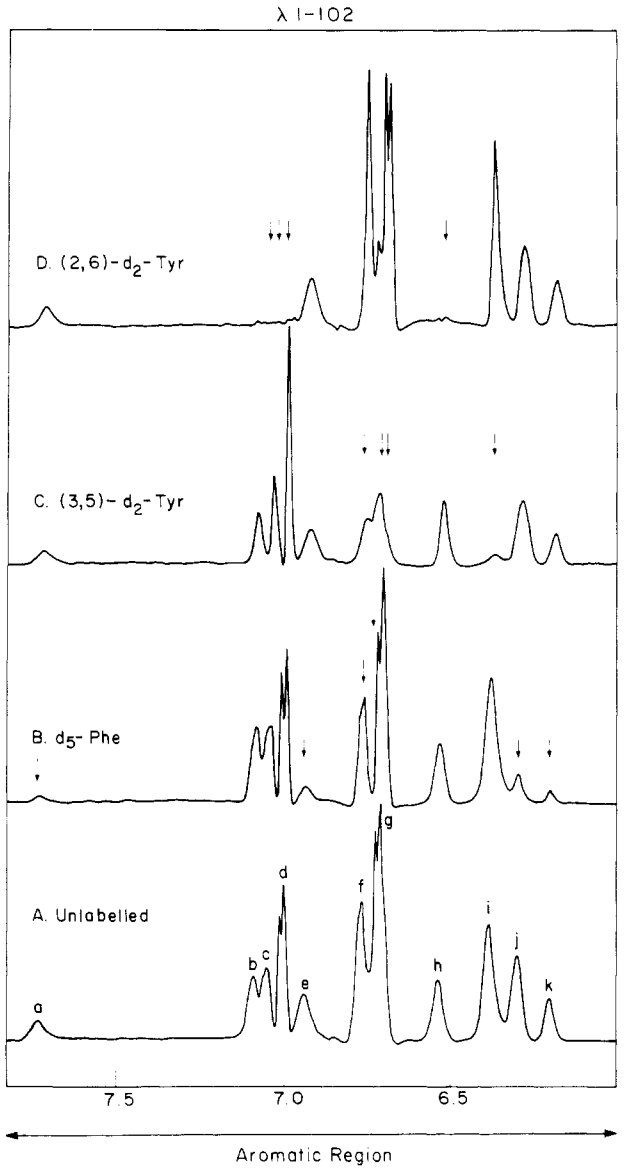

FIGURE 2: Selective incorporation of deuterium labels enables spin systems to be classified by type. Arrows in panels B–D indicate resonances whose amplitude is attenuated by selective deuteration. (A) Aromatic region of the ^{1}H NMR spectrum of the 1–102 fragment at 30 °C and 500 MHz. The resonances are labeled a–k (see Table I). The domain is dimeric at the concentration (5 mM) and conditions used. The spectrum is the sum of 100 scans with a recycle delay of 4 s. A convolution difference with parameters GM4, EM10, and 0.9 was applied. (B) Aromatic spectrum of a 1–102 fragment containing 70% [$^2H_5$]phenylalanine; conditions same as above. (C) Aromatic spectrum of a 1–102 fragment containing [m-$^2H_2$]tyrosine; conditions same as above. (D) Aromatic spectrum of a 1–102 fragment containing [o-$^2H_2$]tyrosine; conditions same as above.

vidually. The assignments obtained are summarized in Table I; the resonances are labeled in panel A of Figure 1.

Tyr-22 and Phe-51. In the crystal structure of the N-terminal domain, Tyr-22 and Phe-51 are partially stacked in the interior (Pabo & Lewis, 1982). Because of their proximity in space, a nuclear Overhauser effect (NOE) is predicted to occur between the protons of these rings. Such an effect would identify their resonances, since no other tyrosine–phenylalanine pair is near enough in the structure to give rise to an observable NOE.

This NOE is shown in Figure 4. Selective irradiation of the para resonance in the upfield-shifted phenylalanine spin system resulted in cross-saturation of the other protons on the same ring and, in addition, of the upfield-shifted tyrosine

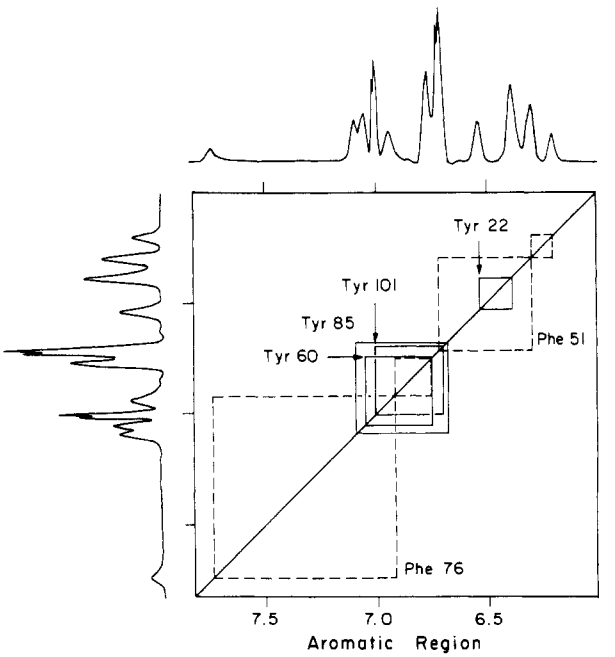

FIGURE 3: Outline of the four tyrosine (solid line) and two phenylalanine (dashed line) spin systems in the aromatic region of the two-dimensional NMR spectrum of the 1–102 fragment. The marked dispersion in chemical shifts reflects the variety of inequivalent magnetic environments in the native structure. Tyr-88 does not appear in the two-dimensional map, since its ortho resonances are broadened by intermediate exchange. The remaining aromatic rings are in fast exchange about the C_β–C_γ bond axis at 0–30 °C. The assignments given are as described in the text and summarized in Table I.

Table I: Aromatic Assignments (Relative to Dioxane at 3.64 ppm)[a]

proton	ppm	peak	proton	ppm	peak
Tyr-22			Tyr-101		
ortho	6.52	h	ortho	7.00	d
meta	6.37	i	meta	6.71	g
Tyr-60			Phe-51		
ortho	7.05	c	ortho	6.74	g
meta	6.77	f	meta	6.29	j
Tyr-85			para	6.19	k
ortho	7.08	b	Phe-76		
meta	6.69	g	ortho	6.75	f
Tyr-88			meta	6.95	e
ortho	6.36	i	para	7.75	a
meta	*b*				

[a] Peak positions refer to panel A of Figure 2. [b] The meta resonance of Tyr-88 is broadened by intermediate exchange.

resonances. These interresidue NOEs are indicated by asterisks in Figure 4. Thus, the upfield-shifted phenylalanine spin system is assigned to Phe-51 and the upfield-shifted tyrosine system to Tyr-22. Their large secondary shifts reflect their stacked geometry in the interior of the protein (Johnson & Bovey, 1958). The assignment of Tyr-22 is confirmed by the study of a mutant domain containing the single amino acid substitution Tyr-22 → His (data not shown).

Phe-76. There are only two phenylalanine residues in the 1–102 domain. Since Phe-51 is assigned to the upfield spin system, Phe-76 is assigned to the downfield spin system. Following selective irradiation of its aromatic resonances, NOEs are observed in the aliphatic region of the spectrum; NOEs involving other aromatic rings are not seen (Weiss et al., 1986). In the crystal structure, Phe-76 projects inward from the turn between helix 4 and helix 5 and is separated from Phe-51 by several buried leucines (Pabo & Lewis, 1982).

The fast exchange character of Tyr-22, Phe-51, and Phe-76 (see above) indicates that there are no significant barriers to ring rotation in the hydrophobic core of the domain. Ring

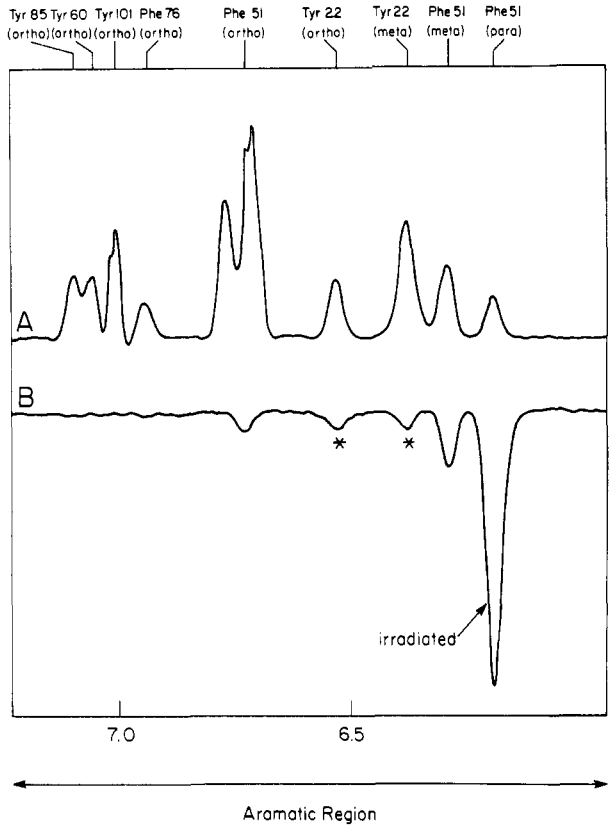

FIGURE 4: One-dimensional nuclear Overhauser effect (NOE) between Phe-51 and Tyr-22 demonstrates their proximity in space. The para resonance of Phe-51 (panel A) was selectively irradiated for 250 ms; the resonance was only half-saturated to avoid nonselective effects. NOEs are observed in the difference spectrum (panel B) to the other protons on the same ring and also to Tyr-22. These interresidue effects are indicated by asterisks. This NOE is to Tyr-22 and not to Tyr-88, whose meta resonance overlaps that of Tyr-22 in the one-dimensional spectrum. Their resonances are resolved in the two-dimensional NOESY spectrum (data not shown). In addition, the Tyr-22–Phe-51 NOE is observed in the Tyr-88 → Cys mutant domain (data not shown). The spectra are the sum of 3400 transients at 30 °C with a recycle delay of 1 s. The NOE difference spectrum was acquired in the interleave mode in blocks of 40. The protein concentration was 5 mM. Spectrum A was processed by convolution difference with parameters GM4, EM10, and 0.9; the difference spectrum was processed by convolution difference with parameters GM10, EM50, and 0.9.

current shift calculations (Johnson & Bovey, 1958; Perkins & Dwek, 1980; Hoch et al., 1982) yield magnetic inequivalences of 0.33 ppm between the ortho protons of Tyr-22 and of 0.28 ppm between its meta protons. This is due primarily to the orientation of Phe-51. Smaller inequivalences are calculated for Phe-51 (<0.07 ppm) and Phe-76 (<0.05 ppm). From the calculated chemical shift differences for Tyr-22, its lifetime with respect to 180° flips about the C_β–C_γ axis can be estimated to be less than 5 ms at 0–30 °C (Wüthrich, 1976).

The resonances from Phe-76 are broader than those from the other internal aromatic rings, Tyr-22 and Phe-51 (see Figure 2). This is not due to ring rotation about the C_β–C_γ bond axis, since the para resonance of Phe-76 is also broadened. Its apparent line width (26 Hz) is 9 Hz larger than that of the para resonance of Phe-51 (17 Hz). This broadening may be due to intermediate exchange between different ring configurations (e.g., ring sliding or rotation about C_α–C_β). Since Phe-76 is positioned in the turn between the globular domain and the dimer helix (see Figure 1B), one possible mechanism for such an exchange would be a hinge-bending motion on a millisecond time scale.

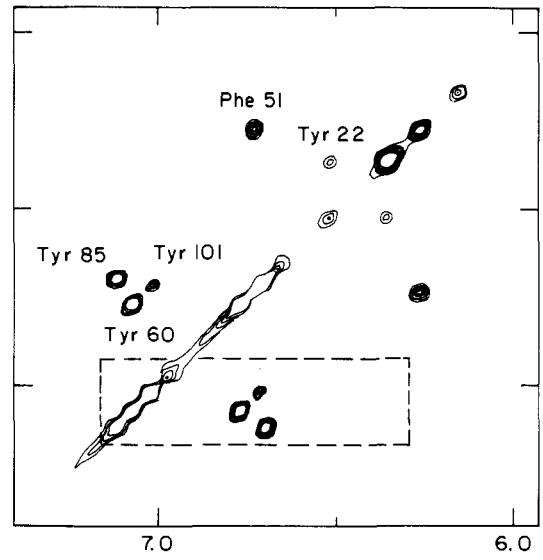

FIGURE 5: Portion of the aromatic region of the two-dimensional Overhauser effect spectrum (NOESY) of the wild-type domain. At the contour levels shown, strong NOEs between ortho and meta protons of the same aromatic ring are observed. The boxed region is shown at lower contours in panel A of Figure 6. This region contains a weak inter-tyrosine NOE. The experiment was performed at 30 °C by the pure-phase method (States et al., 1982). A total of 1024 points was sampled over t_2 with a recycle delay of 1 s. Sixty-four scans were acquired per t_1 value, and 220 t_1 values were obtained. The t_1 dimension was zero-filled to create a square data matrix. A convolution difference with parameters GM10, EM50, and 0.9 was applied in both dimensions. The final data matrix was made symmetrical by minimum value.

Tyr-85 and Tyr-88. Tyr-85 and Tyr-88 are in helix 5. As shown in panel C of Figure 1, Tyr-88 is buried in the dimer contact and is partially stacked against Tyr-88′. Because these two rings are symmetry-related, they give rise to only one set of resonances; accordingly, a Tyr-88–Tyr-88′ nuclear Overhauser effect cannot be observed. Tyr-85 is on the surface of helix 5 and, due to its oblique orientation, approaches within 4 Å of Tyr-88′. Thus, a nuclear Overhauser effect is predicted to occur between these rings (equivalently, between Tyr-85′ and Tyr-88). This is the only inter-tyrosine NOE predicted on the basis of the crystal structure.

The aromatic region of the two-dimensional Overhauser effect spectrum (NOESY) is shown in Figure 5. Strong effects are observed between ortho and meta protons on the same ring, which correspond to correlated spectroscopy (COSY) cross peaks. A unique inter-tyrosine NOE is observed at lower contours, shown in panel A of Figure 6. The ortho protons of one of the tyrosines involved are in intermediate exchange, indicating barriers to ring rotation in its environment. Its meta resonance is identified by selective deuteration (see above). The other tyrosine is in fast exchange. The crystal structure suggests that the constrained ring is Tyr-88 and the unconstrained ring Tyr-85. These assignments are verified through the study of the mutant domains Tyr-85 → Cys and Tyr-88 → Cys described below.

Tyr-101. Tyr-101 may be assigned by comparing the aromatic spectrum of the 1–102 domain with that of a 5–98 domain, as shown in Figure 7. Their similarity implies that removal of the N- and C-terminal residues does not perturb the global folding of the domain (Weiss et al., 1984). One tyrosine spin system is absent in the spectrum of the smaller fragment (the ortho resonance indicated by arrow in Figure 7); this must be Tyr-101. Its meta resonance, poorly resolved near 6.7 ppm, is also absent in the 5–98 spectrum. The resonances of Tyr-101 are observed to be considerably sharper

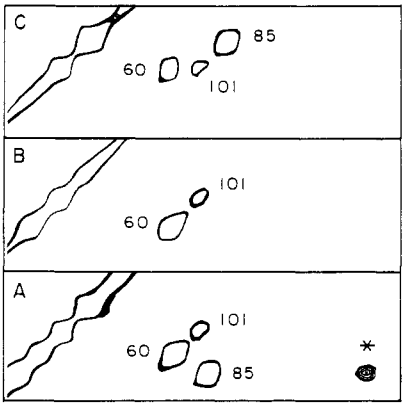

FIGURE 6: (A) Expansion of boxed region in Figure 5 showing unique inter-tyrosine NOE (asterisk). Such an effect is predicted on the basis of the crystal structure (Pabo & Lewis, 1982) between Tyr-88 and Tyr-85′ (equivalently, between Tyr-88′ and Tyr-85), as illustrated in panel B of Figure 1. (B) Corresponding region of the NOESY spectrum of the Tyr-85 → Cys mutant domain under similar conditions. The Tyr-85 spin system is absent, and no inter-tyrosine NOE is observed. Small shifts (<0.02 ppm) are observed in the resonances of Tyr-60. The complete aromatic NOESY spectrum is shown in Figure 11. Experimental conditions are as described in the legend to Figure 5. (C) Corresponding region of the NOESY spectrum of the Tyr-88 → Cys mutant domain. The Tyr-88 spin system is absent, and no inter-tyrosine NOE is observed. The resonances of Tyr-60 and Tyr-85 are shifted upfield and are assigned in the mutant spectrum on the basis of their NOEs with α-protons (Figure 10). Experimental conditions are as described in the legend to Figure 5.

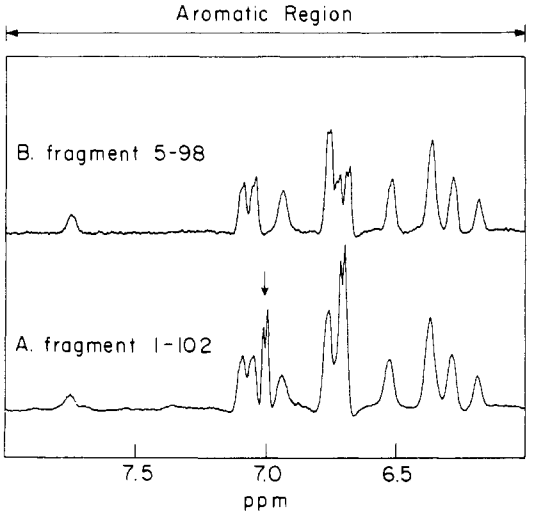

FIGURE 7: Aromatic regions of ^{1}H NMR spectra of the 1–102 (panel A) and 5–98 (panel B) N-terminal domains. The arrow indicates the ortho resonance of Tyr-101. Its meta resonance, which is poorly resolved near 6.7 ppm, is also absent. The proteolytic removal of the N-terminal and C-terminal residues is observed not to perturb the folding of the domain. The spectra were acquired at 30 °C and 500 MHz with a protein concentration of 2.5 mM. Resolution was enhanced by convolution difference with parameters GM4, EM20, and 1.0. The residual HOD signal was presaturated for one s. Spectrum A is the sum of 364 transients with a recycle delay of 2 s. Spectrum B is the sum of 200 transients with a recycle delay of 2 s.

than the other aromatic resonances. A spectrum obtained with the Carr–Purcell–Meiboom–Gill pulse sequence (Campbell et al., 1975) is shown in panel B of Figure 8. This demonstrates that Tyr-101 is in a random-coil state; i.e., local motions (rather than macromolecular rotation) determine its T_2 relaxation.

Tyr-60. Of the five tyrosine spin systems in the ^{1}H NMR spectrum of the domain, four are assigned above. The remaining spin system is assigned to Tyr-60 (see Table I and Figure 3).

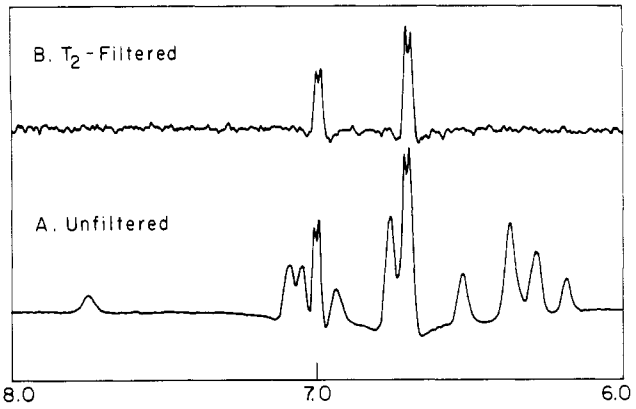

FIGURE 8: Aromatic spectra of the 1–102 fragment (panel A) filtered by T_2 relaxation (panel B). Following 80 ms of transverse relaxation, only the spin system of Tyr-101 is observed. Thus, Tyr-101 is in a random-coil state. Conditions are as described in the legend to Figure 6. Spectrum B was acquired with a Carr–Purcell–Meiboom–Gill sequence (Cambell et al., 1975). During the transverse relaxation period a train of $(\tau-180-\tau)_N$ pulses was applied, with τ = 200 μs and N = 200. The spectrum is the sum of 24 transients with a recycle delay of 5 s.

Table II: Aromatic Assignments (Relative to Dioxane at 3.64 ppm) for Cys-85 and Cys-88 Mutant Domains

proton	Cys-85	Cys-88	proton	Cys-85	Cys-88
Tyr-22			Tyr-101		
ortho	6.52	6.52	ortho	7.00	7.00
meta	6.37	6.37	meta	6.71	6.71
Tyr-60			Phe-51		
ortho	7.06	7.00	ortho	6.74	6.73
meta	6.77	6.77	meta	6.29	6.27
Tyr-85			para	6.19	6.20
ortho		6.92	Phe-76		
meta		6.65	ortho	6.75	6.75
Tyr-88			meta	6.95	6.95
ortho	6.36		para	7.78	7.77
meta	6.52				

Tyr-85 → Cys and Tyr-88 → Cys Mutant Repressors. The residue at position 85 or 88 may be altered by site-directed mutagenesis. Two such genetically altered domains, Tyr-85 → Cys and Tyr-88 → Cys, have been constructed, purified, and characterized (Sauer et al., 1986; Pabo & Suchanek, 1986). The Cys-85 and Cys-88 domains are stably folded and recognize operator DNA. The assignments of Tyr-85 and Tyr-88 given above may be verified by comparison of the spectra of the wild-type and mutant domains. Assignments obtained for the mutant domains are listed in Table II.

In comparing the wild-type and mutant spectra, it is necessary to distinguish resonances that are absent (as a result of the mutation) from resonances that are shifted. This is accomplished by examining the pattern of NOEs between aromatic and nonaromatic protons. The wild-type tyrosine resonances exhibit distinctive NOE patterns in the NOESY spectrum, and these patterns can be used to identify their resonances in the mutant spectra. For example, in the wild-type spectrum shown in Figure 9, Tyr-85 cross-relaxes with two protons in the H_α region, whereas Tyr-60 cross-relaxes with only one proton. These patterns reflect the different environments of the rings in the native structure. Although the H_α resonances have not been assigned, the appearance of the same NOE pattern in the mutant spectra can be used to identify the tyrosines unless nonlocal perturbations occur.

The aromatic spectrum of the Tyr-85 → Cys mutant domain, shown in panel B of Figure 10, is similar to that of wild-type (panel A of Figure 10). The resonances of Tyr-22,

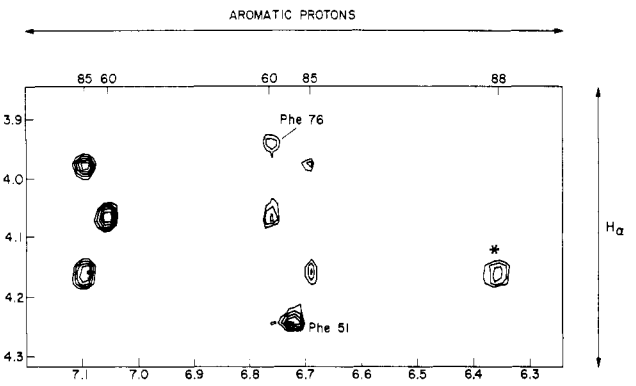

FIGURE 9: The pattern of NOEs between aromatic and nonaromatic protons may be used to distinguish Tyr-60 and Tyr-85. Tyr-60 gives rise to one NOE in the H_α region, whereas Tyr-85 exhibits two NOEs of equal intensity; one of the latter also cross-relaxes with Tyr-88 (asterisk). Conditions are as described in the legend to Figure 5.

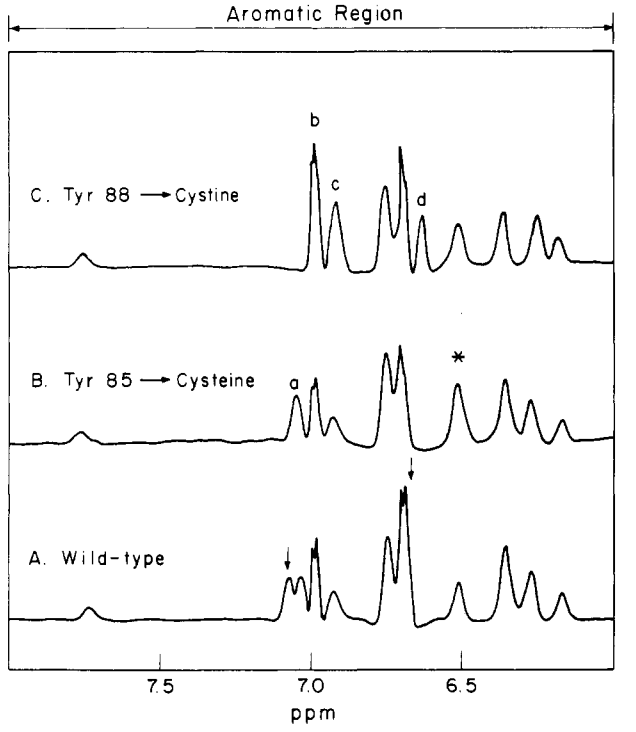

FIGURE 10: Comparison of ^{1}H NMR spectra of wild-type and genetically altered domains. (A) Aromatic spectrum of wild-type 1–102 domain at 500 MHz. Arrows indicate resonances of Tyr-85. The spectrum is the sum of 200 transients with a recycle delay of 4 s. A convolution difference with parameters GM4, EM20, and subtraction factor 1.0 was applied before Fourier transformation. (B) Aromatic spectrum of the reduced form of the Cys-85 mutant domain. Peak a is the ortho resonance of Tyr-60. The asterisk indicates the ortho resonance of Tyr-88, which overlaps that of Tyr-22. The spectrum is the sum of 216 transients with a recycle delay of 4 s. A convolution difference with parameters GM4, EM20, and 1.0 was applied. (C) Aromatic spectrum of the Cys-88 covalent dimer. Peak b contains the ortho resonances of Tyr-60 and Tyr-101. Peak c contains the ortho resonance of Tyr-85 and the meta resonance of Phe-76. Peak d is the meta resonance of Tyr-85. Assignments for the mutant domains are given in Table II. These spectra were recorded at 30 °C and 500 MHz with protein concentration at 5 mM. Resolution was enhanced by convolution difference with parameters GM4, EM20, and 1.0. The residual HOD signal was presaturated for 1 s. Spectrum A is the sum of 200 transients with a recycle delay of 4 s. Spectrum B is the sum of 216 transients with a recycle delay of 4 s. Spectrum C is the sum of 604 transients with a recycle delay of 1.5 s.

Phe-51, and Phe-76 are nearly identical in the mutant and wild-type spectra (relative chemical shift differences less than 0.03 ppm), indicating that the tertiary structure of the domain is not perturbed by the mutation. The two-dimensional Overhauser spectrum of the Cys-85 domain is shown in Figure 11. One tyrosine spin system is absent in the mutant spectrum; this must be Tyr-85 (indicated by arrows in panel A of Figure 10). A small shift (<0.02 ppm) is observed in the ortho resonance of Tyr-60 (peak b in Figure 10B). This may be due either to the absence of the Tyr-85 diamagnetic field or to structural effects of the mutation. The meta resonance of Tyr-60 is not perturbed (panels A and B of Figure 6). No inter-tyrosine NOE is observed, as shown in panel B of Figure 6. In the mutant domain, Tyr-60 exhibits the same pattern of nonaromatic NOEs as in the wild type (data not shown).

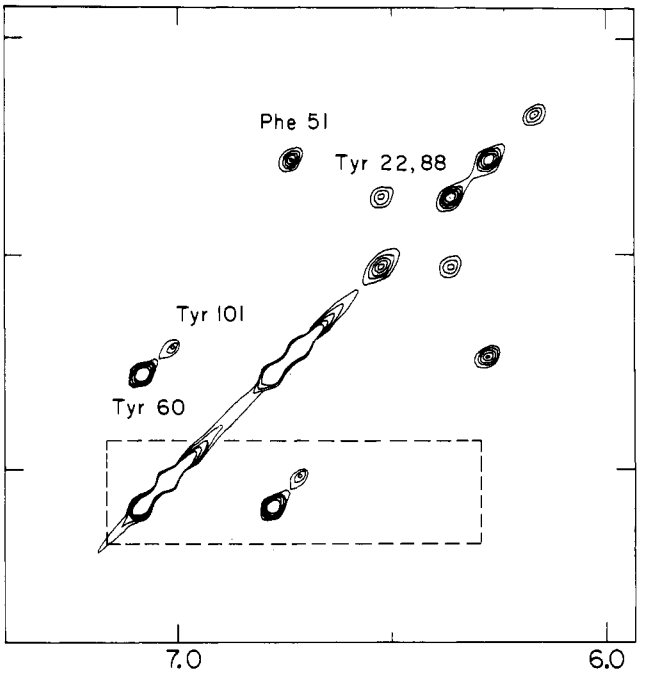

FIGURE 11: Portion of the aromatic region of the two-dimensional Overhauser effect spectrum (NOESY) of the Cys-85 mutant domain. Contours shown correspond to those in Figure 5 and demonstrate that one tyrosine spin system is absent. This is assigned to Tyr-85 in the wild-type spectrum. A small shift (<0.02 ppm) is observed in the ortho resonance of Tyr-60. The boxed region is shown at lower contours in panel B of Figure 6. Conditions are as described in the legend to Figure 5.

An additional feature of the mutant spectrum is observed near 6.5 ppm. This resonance, which overlaps the ortho resonance of Tyr-22, is indicated by an asterisk in panel B of Figure 10. It is assigned to the ortho protons of Tyr-88, the only protons whose resonances are not observed in the wild-type spectrum. Thus, these protons are in fast (rather than intermediate) exchange in the mutant spectrum. This change in exchange character implies either an increase in the rate of ring rotation or a decrease in local magnetic inequivalence. The latter mechanism is unlikely, since the chemical shift of the Tyr-88 meta resonances is unperturbed in the mutant. Presumably, Tyr-85′, hinders the rotation of Tyr-88, and its replacement by a smaller side chain reduces the barrier to ring rotation. These changes in the dynamics apparently do not involve nonlocal structural perturbations (Shih et al., 1985). Similar effects have been observed in a reduced form of bovine pancreatic trypsin inhibitor (States et al., 1984) and are consistent with mechanisms proposed for ring rotation (Karplus & McCammon, 1983), in which van der Waals interactions are dominant.

The aromatic spectrum of a Tyr-88 → Cys mutant domain is shown in panel C of Figure 10. This cysteine spontaneously forms an intermolecular disulfide bond with Cys-88′. This is in contrast to the Cys-85 mutant discussed above, which does

not contain a disulfide bond (Sauer et al., 1986). The resonances of Tyr-22 and Phe-51 are almost identical with those of the wild type (relative chemical shift differences less than 0.02 ppm), indicating as above a correspondence of tertiary structure. A small shift (0.03 ppm) is observed in the para resonance of Phe-76; this may reflect a change in the configuration of the loop between helix 4 and helix 5. The Tyr-88 resonances are absent, consistent with the amino acid substitution. No inter-tyrosine NOEs are observed in the two-dimensional NOESY spectrum of the mutant domain, as shown in panel C of Figure 6. The resonances of Tyr-60 and Tyr-85 are shifted upfield relative to their positions in the wild-type spectrum (peaks b–d) and are assigned on the basis of NOEs involving nonaromatic protons (e.g., H_α protons as described above). Larger shifts are observed for Tyr-85 (0.2 ppm) than for Tyr-60 (0.05 ppm), which is consistent with their relative distance from the missing Tyr-88 ring. These shifts may reflect either ring current effects (Johnson & Bovey, 1958) or perturbations in the structure of the dimer contact.

Discussion

The primary objective of this paper is the assignment of the aromatic ^{1}H NMR spectrum of the operator binding domain of λ repressor. This spectrum consists of five tyrosines and two phenylalanines in the 1–102 fragment. Since the resonances of this 23-kDa domain are too broad for the application of two-dimensional strategies for sequence-specific assignment (Wüthrich et al., 1982; Weber et al., 1985), an alternative approach has been used. By a combination of one- and two-dimensional NMR methods, comparisons with the crystal structure, biosynthetic incorporation of deuterium labels, and the study of genetically altered domains, it has been possible to obtain a complete assignment of the aromatic spectrum.

The aromatic ^{1}H NMR resonances provide sensitive markers for both tertiary and quaternary structure. Tyr-22, Phe-51, and Phe-76 are buried in the hydrophobic interior of the domain. Their resonances exhibit large upfield and downfield shifts, which arise from tertiary interactions in the folded state of the protein. Because large magnetic gradients are calculated to occur in their local environments (Johnson & Bovey, 1958), the ^{1}H NMR resonances of these rings should be sensitive to small perturbations in tertiary structure. Likewise, the resonances of Tyr-85 and Tyr-88, which are located in the dimer contact, provide markers for perturbations in quaternary structure.

Nuclear Overhauser effects demonstrate that the major features of the crystal structure are retained in solution. NOEs expected from the crystal structure (e.g., Tyr-85–Tyr-88′) are observed, whereas those not predicted (e.g., Phe-51–Phe-76) are not observed. In particular, an NOE is observed between Tyr-22 and Phe-51, indicating their proximity in solution in accord with the crystal structure. Their resonances are unperturbed in the Cys-85 and Cys-88 mutant domains, indicating that these mutations in helix 5 do not distort the tertiary structure of the domain. Dynamical features of the wild-type and mutant domains are also observed. The globular region of the domain, consisting of the first four helices, is not rigid, as demonstrated by the absence of significant barriers to ring rotation. The *lac* repressor headpiece is also a loose structure in solution (Buck et al., 1981; Wade-Jardetzky et al., 1979; Jarema et al., 1981; Zuiderweg et al., 1983; Kaptein et al., 1985). The resonances of Phe-76 are broader than the other internal rings; one possible explanation is that the ring is in intermediate exchange between different orientations involving displacements of all protons; a single rotation about C_β–C_γ is not sufficient. Barriers to ring rotation are observed for Tyr-88, which is stacked against the symmetry-related ring in the dimer interface. A NOE is observed between Tyr-88 and Tyr-85′ (equivalently, between Tyr-88′ and Tyr-85); this interaction appears to contribute to constraining the rotation of Tyr-88, since replacement of Tyr-85 by a smaller residue (cysteine) reduces this barrier. No barriers are observed for Tyr-85.

We anticipate that the ^{1}H NMR assignments described here will provide valuable markers for additional experimental studies of wild-type and genetically altered λ repressors (Nelson et al., 1983; Hecht et al., 1983) and for the analysis of their interaction with operator DNA.

Acknowledgments

We thank Carl Pabo and Mitch Lewis for the crystal coordinates of λ repressor and helpful discussion; Anna Jeitler-Nilsson and Kathy Hehir for help with protein purification; Robert Stearman, Michael Hecht, and Hillary Nelson for mutant plasmids; Jeff Hoch for assistance in calculating ring current shifts; Dinshaw Patel, David States, David Ruben, Ponzy Lu, and Alfred Redfield for advice regarding NMR techniques; and Anne Lawthers for preparation of the manuscript. The 500-MHz spectra were recorded at the High-Field NMR Resource of the Francis Bitter National Magnet Laboratory (NIH, RR-00995).

References

Anderson, J., Ptashne, M., & Harrison, S. C. (1984) *Proc. Natl. Acad. Sci. U.S.A. 81*, 1307–1311.

Aue, W. P., Bartholdi, E., & Ernst, R. R. (1976) *J. Chem. Phys. 64*, 2229–2241.

Buck, F., Returjans, H., & Beyreuther, K. (1978) *FEBS Lett. 96*, 335–338.

Cambell, I. D., Dobson, C. M., Williams, R. J. P., & Wright, P. E. (1975) *FEBS Lett. 57*, 96–99.

DeAnda, J., Poteete, A. R., & Sauer, R. T. (1983) *J. Biol. Chem. 258*, 10536–10542.

Gupta, R. K., & Redfield, A. G. (1971) *Cold Spring Harbor Symp. Quant. Biol. 36*, 405–413.

Hecht, M. H., Nelson, H. C. M., & Sauer, R. T. (1983) *Proc. Natl. Acad. Sci. U.S.A. 80*, 2676–2680.

Hoch, J. C., Dobson, C. M., & Karplus, M. (1982) *Biochemistry 21*, 1118–1125.

Jarema, M. A. C., Lu, P., & Miller, J. H. (1981) *Proc. Natl. Acad. Sci. U.S.A. 78*, 2707–2711.

Jeener, J. (1971) *Ampere International Summer School XI*, Basko, Polje, Yugoslavia.

Johnson, C. E., & Bovey, F. A. (1958) *J. Chem. Phys. 29*, 1012–1014.

Kaptein, R., Zuiderweg, E., Scheck, R. M., Boelens, R., & Van Gunsteren, W. F. N. (1985) *J. Mol. Biol. 182*, 179–182.

Karplus, M., & McCammon, J. A. (1983) *Annu. Rev. Biochem. 52*, 263–300.

Nelson, H. C. M., Hecht, M. H., & Sauer, R. T. (1983) *Cold Spring Harbor Symp. Quant. Biol. 47*, 441–449.

Pabo, C. O., & Lewis, M. (1982) *Nature (London) 298*, 443–447.

Pabo, C. O., & Suchanek, E. (1986) *Biochemistry 25*, 5987–5991.

Pabo, C. O., Sauer, R. T., Sturtevant, J., & Ptashne, M. (1979) *Proc. Natl. Acad. Sci. U.S.A. 76*, 1608–1612.

Perkins, S. J., & Dwek, R. A. (1980) *Biochemistry 19*, 245–258.

Platt, T., Files, J., & Weber, K. (1973) *J. Biol. Chem. 248*, 110–121.

Sauer, R. T., & Anderegg, R. (1978) *Biochemistry 17*, 1092–1100.
Sauer, R. T., Pabo, C. O., Meyer, B. J., Ptashne, M., & Backman, K. C. (1979) *Nature (London) 279*, 396–400.
Sauer, R. T., Hehir, K., Stearman, R. S., Weiss, M. A., Jeitler-Nilsson, A., Suchanek, E. G., & Pabo, C. O. (1986) *Biochemistry 25*, 5992–5998.
Shih, H. H.-L., Brady, J., & Karplus, M. (1985) *Proc. Natl. Acad. Sci. U.S.A. 82*, 1697–1701.
States, D. J., Haberkorn, R. A., & Ruben, D. J. (1982) *J. Magn. Reson. 48*, 286–292.
States, D. J., Dobson, C. M., Karplus, M., & Creighton, T. E. (1984) *J. Mol. Biol. 174*, 411–418.
Wade-Jardetzky, N., Bray, R. P., Conover, W. W., Jardetzky, O., Geisler, N., & Weber, K. (1979) *J. Mol. Biol. 128*, 259–264.
Wagner, G., & Wüthrich, K. (1982) *J. Mol. Biol. 155*, 347–366.
Weber, K., & Geisler, N. (1978) in *The Operon* (Miller, J., & Reznikoff, W., Eds.) pp 155–163, Cold Spring Harbor Press, Cold Spring Harbor, NY.
Weber, P. L., Drobny, G., & Reid, B. R. (1985) *Biochemistry 24*, 4549–4552.
Weiss, M. A., Karplus, M., Patel, D. J., & Sauer, R. T. (1983) *J. Biomol. Struct. Dyn. 1*, 151–157.
Weiss, M. A., Sauer, R. T., Patel, D. J., & Karplus, M. (1984) *Biochemistry 23*, 5090–5095.
Weiss, M. A., Redfield, A. G., & Griffey, R. H. (1986) *Proc. Natl. Acad. Sci. U.S.A. 83*, 1325–1329.
Weiss, M. A., Pabo, C. O., Karplus, M., & Sauer, R. T. (1987) *Biochemistry* (following paper in this issue).
Wüthrich, K. (1976) *NMR in Biological Research: Peptides and Proteins*, Elsevier, New York.
Wüthrich, K., Wider, G., Wagner, G., & Braun, W. (1982) *J. Mol. Biol. 155*, 311–319.
Zuiderweg, E. R., Kaptein, R., & Wüthrich, K. (1983) *Proc. Natl. Acad. Sci. U.S.A. 80*, 5837–5841.

Dimerization of the Operator Binding Domain of Phage λ Repressor†

Michael A. Weiss,‡,§ Carl O. Pabo,‖ Martin Karplus,*,‡ and Robert T. Sauer⊥

Department of Chemistry, Harvard University, Cambridge, Massachusetts 02138, Department of Medicine, Brigham and Women's Hospital, Boston, Massachusetts 02115, Department of Biophysics, The Johns Hopkins School of Medicine, Baltimore, Maryland 21205, and Department of Biology, Massachusetts Institute of Technology, Cambridge, Massachusetts 02139

Received June 10, 1986; Revised Manuscript Received September 19, 1986

ABSTRACT: Dimerization of λ repressor is required for its binding to operator DNA. As part of a continuing study of the structural basis of the coupling between dimer formation and operator binding, we have undertaken ^{1}H NMR and gel filtration studies of the dimerization of the N-terminal domain of λ repressor. Five protein fragments have been studied: three are wild-type fragments of different length (1–102, 1–92, and 1–90), and two are fragments bearing single amino acid substitutions in residues involved in the dimer interface (1–102, Tyr-88 → Cys; 1–92, Ile-84 → Ser). The tertiary structure of each species is essentially the same, as monitored by the ^{1}H NMR resonances of internal aromatic groups. However, significant differences are observed in their dimerization properties. ^{1}H NMR resonances of aromatic residues that are involved in the dimer contact allow the monomer–dimer equilibrium to be monitored in solution. The structure of the wild-type dimer contact appears to be similar to that deduced from X-ray crystallography and involves the hydrophobic packing of symmetry-related helices (helix 5) from each monomer. Removal of two contact residues, Val-91 and Ser-92, by limited proteolysis disrupts this interaction and also prevents crystallization. The Ile-84 → Ser substitution also disrupts this interaction, which accounts for the severely reduced operator affinity of this mutant protein.

The λ repressor regulates gene expression by binding, as a dimer, to specific sequences of operator DNA (Chadwick et al., 1971; Johnson et al., 1980). Because dimer formation and DNA binding are coupled equilibria, dimerization contributes to apparent operator affinity. The intact repressor has not been crystallized, but studies of isolated proteolytic fragments suggest that there are two sets of dimer contacts; an N-terminal fragment (residues 1–92) crystallizes as a dimer (Pabo & Lewis, 1982), and a C-terminal fragment (residues 93–236) dimerizes readily in solution (Pabo et al., 1979). The N-terminal domain of repressor appears to mediate all of the contacts with operator DNA (Sauer et al., 1979), but it is likely that both N-terminal and C-terminal quaternary interactions contribute to the strength of operator binding. The importance of the C-terminal contacts has been inferred from the finding that intact repressor binds operator DNA at concentrations about 100-fold lower than those required to observe operator binding by N-terminal fragments. The importance of N-terminal dimerization has been inferred from the operator DNA protection patterns exhibited by N-terminal fragments (Sauer et al., 1979; Johnson, 1980), from consid-

† This work was supported in part by grants from the National Institutes of Health to M.K. (GM-37292), C.O.P. (GM-31471), and R.T.S. (AI-15706).
‡ Harvard University.
§ Brigham and Women's Hospital.
‖ The Johns Hopkins School of Medicine.
⊥ Massachusetts Institute of Technology.

0006-2960/87/0426-0897$01.50/0